J. Astron. Space Sci. 11(1), 1-12 (1994)

MAGNETOSPHERIC STRUCTURE OF THE INTERMEDIATE POLAR

Yonggi Kim
Yonsei University Observatory
Seoul 120-749, Korea
email: mira@bubble.yonsei.ac.kr

(Received May 19, 1994; Accepted June 8, 1994)

ABSTRACT

The structure of the magnetic funnel element in the intermediate polar is considered in terms of an important site for the X-ray absorption and the reemission of the X-ray as the optical light. In this paper the column density and the optical depth vary with the filling factor, which is introduced to characterize the structure of matter in the magnetic funnel element. The results of the energy dependence of the X-ray spectrum and the modulation depth of the X-ray light curve are discussed.

1. INTRODUCTION

Recently, the physics of the accretion from the accreton disc into the surface of the intermediate polar via the magnetosphere have been studied by several authors (Rosen *et al.* 1991, Kim 1992, Ferrario *et al.* 1993). A theoretical foundation of these studies originates from Ghosh and Lamb (1979a, b), who divided the accretion flow into four regions: an unpertubed disc, an outer transition zone, an inner transition zone, and a magnetosphere. The material passing through the Lagrangian point forms an accretion disc, which, at some radius, is disturbed by the magnetic field of the white dwarf. Up to the outer transition zone, the material is essentially in Keplerian motion. In the inner transition zone, the magnetic stress changes the angular velocity from Keplerian to corotaional. At some radius of the magnetosphere, the magnetic stress is so great that the material starts to accrete along the magnetic field line.

It is not clear until now in which form the material accretes to the stellar surface through the magnetosphere. Because the X-rays produced near the stellar surface seem to pass this infalling material in the magnetosphere and to be absorbed, it is very important to know the structure of this material. Rosen *et al.* (1988) proposed

a tall, thin column in the magnetosphere. The large-scale flow along the field line into the stellar surface is postulated to act as an accretion curtain, modulating X-rays by varying the photoelectric absorption. Similar to this model, Kim (1992) and Kim and Beuermann (1994a,b) have developed a phenomenological model of X-rays and optical spectrum.

In this paper, we consider the structure of the absorbing material infalling to the stellar surface along the magnetic field, which can explain the observed X-ray photoabsorption and the optical spectrum reprocessed in the magnetic funnel elements. A filling factor of the funnel elements is introduced for this purpose and the variation of the X-rays with filling factor is discussed in detail. In order to explain the optical spectrum and optical line emission, we used the optical thin as well as the optical thick funnel elements. We modified the accretion curtain model by assuming that the material in the magnetic funnel elements consists of many optical thick blobs. It can be seen that this modified model provides a natural explanation of the observed properties of the radiations.

2. THE FATE OF THE X-RAY RADIATION

The magnetospheric property of the cataclysmic variables is generally characterized by the ratio of the magnetospheric radius and separation distance, $\frac{r_M}{r_a}$. For the intermediate polar, the relation of $R_{wd} < r_M < \frac{1}{2}r_a$ is thought to be valid, and the rotation period and orbital period are not same ($\omega_1 \neq \Omega$). This situation is illustrated in Figure 1a. The accretion disc is penetrated by the magnetosphere, where $r < r_M$, and the material starts to accrete on the pole of the white dwarf along the magnetic field. Near the upper and lower pole of the magnetic field, the accretion energy is thermalized by shock and radiates X-ray as a result. The intensity of the X-ray radiation seems to be given by the integration of the volume emissivity ϵ_ν of the thermal bremsstrahlung:

$$\begin{aligned} L_\nu &= 4\pi \int \epsilon_\nu dV \\ &= 5.57 \times 10^{22} M_1 \dot{M}_{16} R_9^{-1} T^{-1/2} g(\nu, T) e^{-\frac{h\nu}{kT}} \\ &\quad erg\, s^{-1} Hz^{-1}, \end{aligned} \tag{1}$$

where M_1 is the mass of the white dwarf in solar unit, $\dot{M}_{16}$ is the accretion rate in $10^{16} g\, s^{-1}$, R_9 is the radius of white dwarf in $10^9 cm$, T_λ is the shock temperatur, and $g(\nu, T)$ is the gaunt factor.

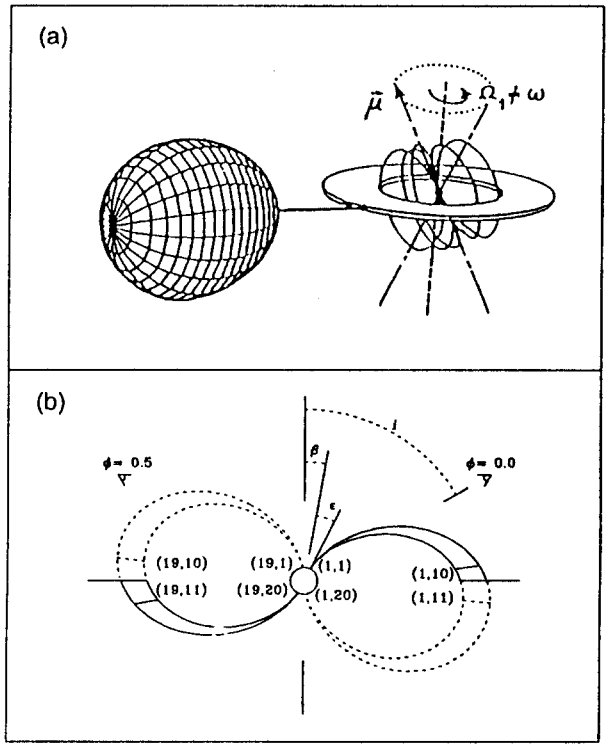

Figure 1. Configuration of magnetosphere and accretion disc in the intermediate polar. a) presents a schematic geometry of this configuration, while b) presents a side on view of a simple dipole magnetic geometry.

In order to study the fate of this X-ray radiation it is assumed here that the magnetic field of the white dwarf is given by dipole as a first approximation. The accretion of the material then occures in the confined region in the magnetosphere as can be seen in Figure 1b. The X-ray source is divided into 72 point sources (36 point sources over the upper and lower pole respectively) and the accretion region at a given azimuth angle is divided into 20 elements.

An absorber with a density ρ at the distance of r from the source experiences the intensity

$$I_{0,\nu} = \frac{L_\nu}{4\pi r^2}\, erg\, s^{-1} cm^{-2} \tag{2}$$

and for the absorption length l, the column density and the optical depth are then given by

$$N_H = \rho l \, cm^{-2} \tag{3}$$

$$\tau = \sigma_H N_H. \tag{4}$$

Among the radiation energy of the i-th point source incoming to this absorber with the area A, $I_{0,\nu} A d\nu$, only some fraction can reach to the observer because of the photoabsorption:

$$I_{\nu,i} = I_{0,\nu} e^{-\sigma_\nu N_H}. \tag{5}$$

The another part is absorbed in this absorber. The absorbed X-ray energy can be written by

$$E_{\nu,i} = \int I_{0,\nu}(1 - e^{-\sigma_\nu N_H}) A d\nu \quad erg\, s^{-1}. \tag{6}$$

Our model assumes as the next step that the absorbed energy is reradiated in the optical region (reprocessing of the X-ray radiation). This reprocessed radiation at one accretion funnel element can be characterized by the black body radiation, and its effective temperature is given by the summation of the absorbed energy for every 72 point sources:

$$\sum_{k=1}^{36} \sum_{m=1}^{36} \frac{E_{\nu,k} + E_{\nu,m}}{2A} = \sigma T_{eff}^4 \tag{7}$$

In this equation k and m denote the sources around the upper and lower pole, respectively. Using this effective temperature, a model atmosphere (Kurucz 1979) has been calculated for the optical spectrum. The result of this calculation shows at first that all of the funnel elements are optically thin so that the continuum spectrum requiring the optically thick elements can not be explained by this model. In the following, we therefore suggest a possibility to improve this problem in the intermediate polar.

3. FILLING FACTOR AND ABSORPTION PROBABILITY

In order to explain the optically thick continuum radiation, it is assumed here that the accretion funnel consists of many of thin filaments containing the optically

thick material. The diameter and density of this filament are denoted by a and ρ_0 in Figure 2. With the number of filaments pro unit of area, k, the filling factor defined as the occupied area pro unit of area can now be described by

$$f = k \times a^2 = \frac{\rho_0}{\rho}. \tag{8}$$

There are then $l \times k$ filaments in the absorption length l with this structure. The actual absorption length b can be then calculated for the two cases:

$$b = \begin{cases} a & : \; l \times k \times a \leq 1 \\ l \times f & : \; l \times k \times a > 1. \end{cases} \tag{9}$$

Equations (8) and (9) allow us to estimate the column density of this absorber for the case of $l \times k \times a > 1$:

$$N_H = b \times \frac{\rho}{m_p} = N_{H,0} \frac{1}{f \times fx}. \tag{10}$$

Here a new parameter fx is introduced by $fx = \frac{l}{a}$, and $N_{H,0}$ is the column density of one filament.

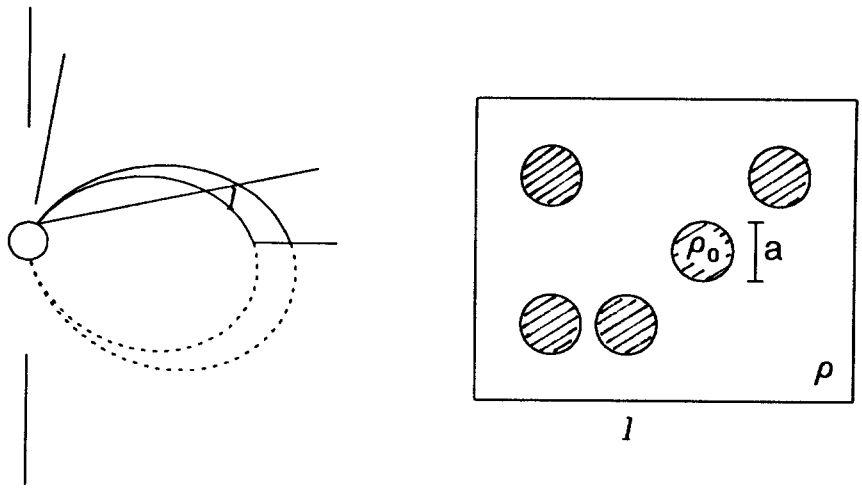

Figure 2. Schematic geometry of a funnel element. The geometric length and density of the funnel element amount to l and ρ, while a and ρ_0 for a filament.

We define an absorption probability W which can give approximately the column density of an absorber for the both cases of eq. (9):

$$W = 1 - e^{-f \times fx}. \tag{11}$$

With this absorption probability W, the column density of one absorber can be rewritten for the both case of eq. (9) by

$$N_H = \frac{N_{H,0}}{W}. \tag{12}$$

In Figure 3 the functions of eqs. (9), (11) and (12) are illustrated graphically. The new two parameters, f and fx, have been applied to the calculation of photoabsorption of X-rays and its reprocessing in the funnel element. The definition of the filling factor, that only the fraction f of the absorber can absorb the X-ray radiation, distinguishes two ways for the fate of X-ray radiation. Namely (1-f) of the incoming X-ray radiation passes the absorber without experiencing absorption, while f of the incoming radiation goes with absorption through the accretion funnel. The X-ray radiation reaching to the observer after absorption consists now of two parts in contrast to eq. (5):

$$I_{\nu,i} = I_{0,\nu} f e^{-\sigma_\nu N_H} + I_{0,\nu}(1 - f). \tag{13}$$

The absorbed energy must be also rewritten according to the change of the funnel structure:

$$E_{a,i} = \int I_{\nu,i}(1 - e^{-\sigma_\nu N_H}) f A d\nu \quad ergs^{-1}, \tag{14}$$

where N_H in the above equations is given by eq. (12); therefore different from N_H in eq. (5). With the effective absorption area $A \times f$ and the renewed $E_{a,i}$ in eq. (14), the effective temperature can then be calculated as in eq. (7).

The result of the calculation explains the optically thick and optically thin part of the accretion funnel naturally. In table 1, some results for the optical depth of the accretion funnel innerpart and outerpart of the magnetosphere calculated with the model parameter in Kim and Beuermann (1994a) have been represented. One can see from this table that our model with absorption probability is able to provide an optically thick accretion funnel element as well as an optically thin element. It can now be suggested that the continuum spectrum resulted from the optically thick element is produced near the magnetic pole, while the outer part of the magnetosphere is responsible for the line emission.

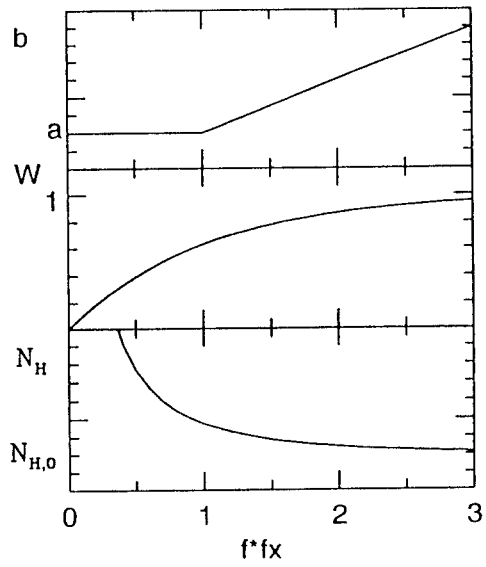

Figure 3. The actual absorption length, absorption probability and the column density as a function of the new introduced parameters, $f \times fx$.

4. RESULTS AND DISCUSSION

It has been shown in previous section that our model with the absorption probability can reproduce the observed X-ray and optical spectrum. This result can be applied to estimate the model parameter by comparing our calculated spectrum with the observed spectrum. Such comparison will be presented elsewhere. Some light curves of X-ray and optical spectrum calculated with our model demonstrate how good our model calculation can reproduce the observational data qualitatively.

The observed X-ray spectrum of the intermediate polar indicates the dependence on the photon energy in rotational phase (Rosen *et al.* 1988, Beuermann 1988, Hellier *et al.* 1991). The X-ray light curves have been therefore calculated for some energy bands, and illustrated in Figure 4. The observed X-ray light curves of EX Hya adopted from Rosen *et al.* (1988) are also presented in this figure.

In order to analyze the X-ray light curve, a modulation depth F_m is defined by

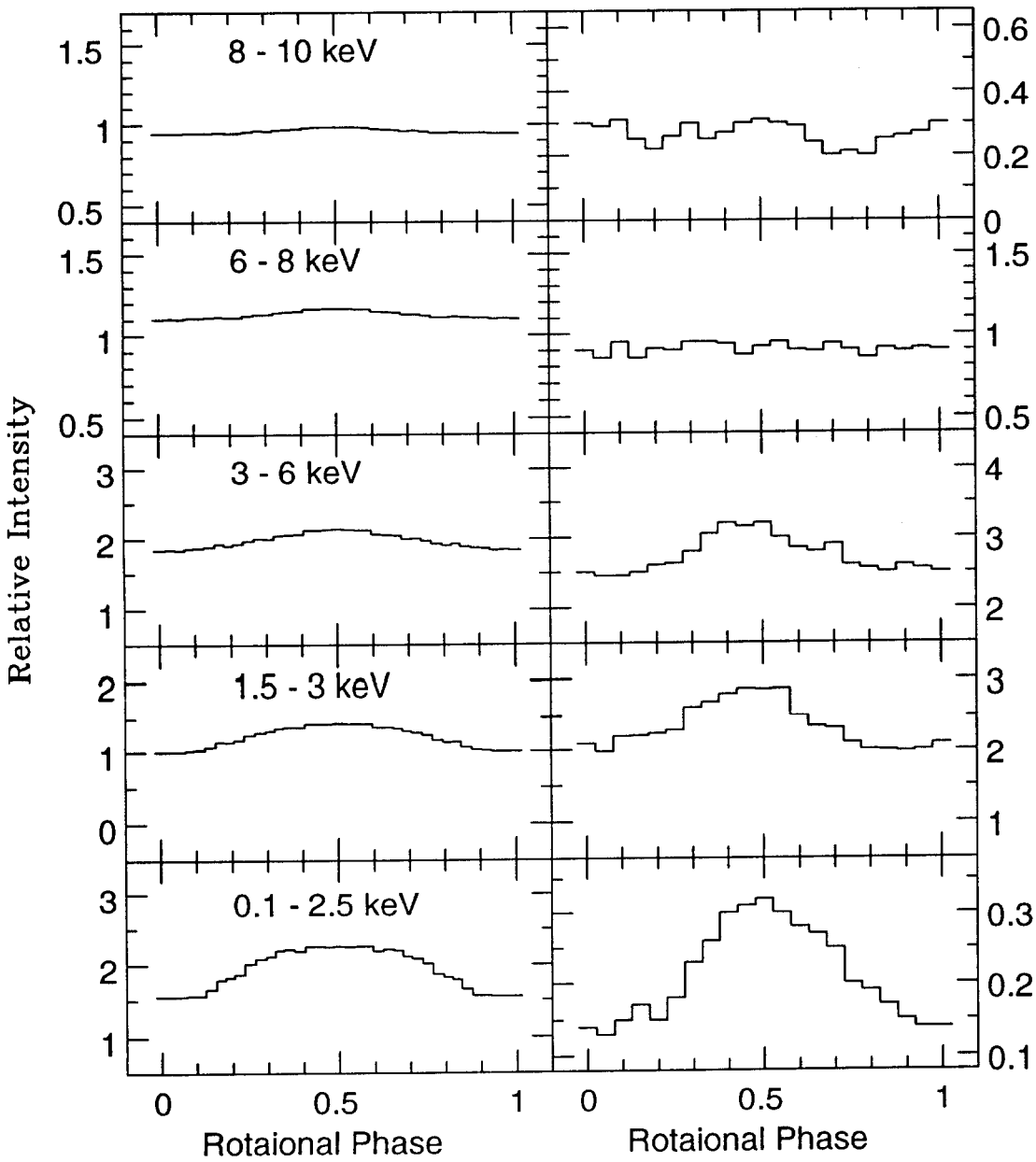

Figure 4. Calculated (left) and observed (right) X-ray light curves of EX Hya. The observed data are adopted from Rosen *et al.* (1988).

Table 1. Optical depth of the outside and inside funnel elements, τ_{10} and τ_1, for some model parameters used for the calculation of X-ray and optical spectrum.

fx	f	$\dot{M}_{16}$	τ_{10}	τ_1
1	0.5	1	3.32×10^{-3}	2.35×10^{-2}
1	0.1	1	3.39×10^{-3}	2.5
1	0.1	3	1.50×10^{-2}	13
1	0.1	4	2.30×10^{-2}	20
2	0.1	4	1.57×10^{-2}	11
3	0.1	4	1.26×10^{-2}	7.5

$$F_m = \frac{S_{max} - S_{min}}{S_{max}} \times 100, \tag{15}$$

where S_{max} and S_{min} are the maximum and minimum flux in the light curve at a given energy. The calculate modulation depthes of the light curves presented in Figure 3 are 31.1, 30.1, 13.9, 5 and 4 % for 0.01 - 2.5, 1.5 - 3, 3 - 6, 6 - 8, 8 - 10 keV respectively. The observed modulation depthes of X-ray light curves of EX Hya amount to 43.5, 19, 10, 5.8 and 6 % for the same energy band respectively. The observed light curve of 8 - 10 keV indicates no clear dependence on rotational period. It is probably caused by the contamination of the hard X-ray component which is independent on energy and rotaional period as discussed in Rosen *et al.* (1991).. This comparison shows that our model can provide a set of light curves compatible to the observed data. Model fitting of the observed data is in progress and will be presented elsewhere.

Some optical light curves are also calculated and illustrated in Figure 5. In this figure, light curves for the intensity of continuum and $H\beta$ line emission as well as the equvalent width and V/R ratio of the $H\beta$ line profile are presented. The equivalent width of a line profile is defined as a width of rectangle in line center, which area is same as the integrated area of the profile relativ to the continuum flux:

$$W_\lambda = \frac{\int (S_L(\lambda) - S_C) d\lambda}{S_C}, \tag{16}$$

where S_C is the flux of continuum which is estimated by the averaging the flux at the end of the both line wings. The V/R ratio is defined as the ratio of the equivalent width of left part to the right part of the line profile. A study of this ratio can provide

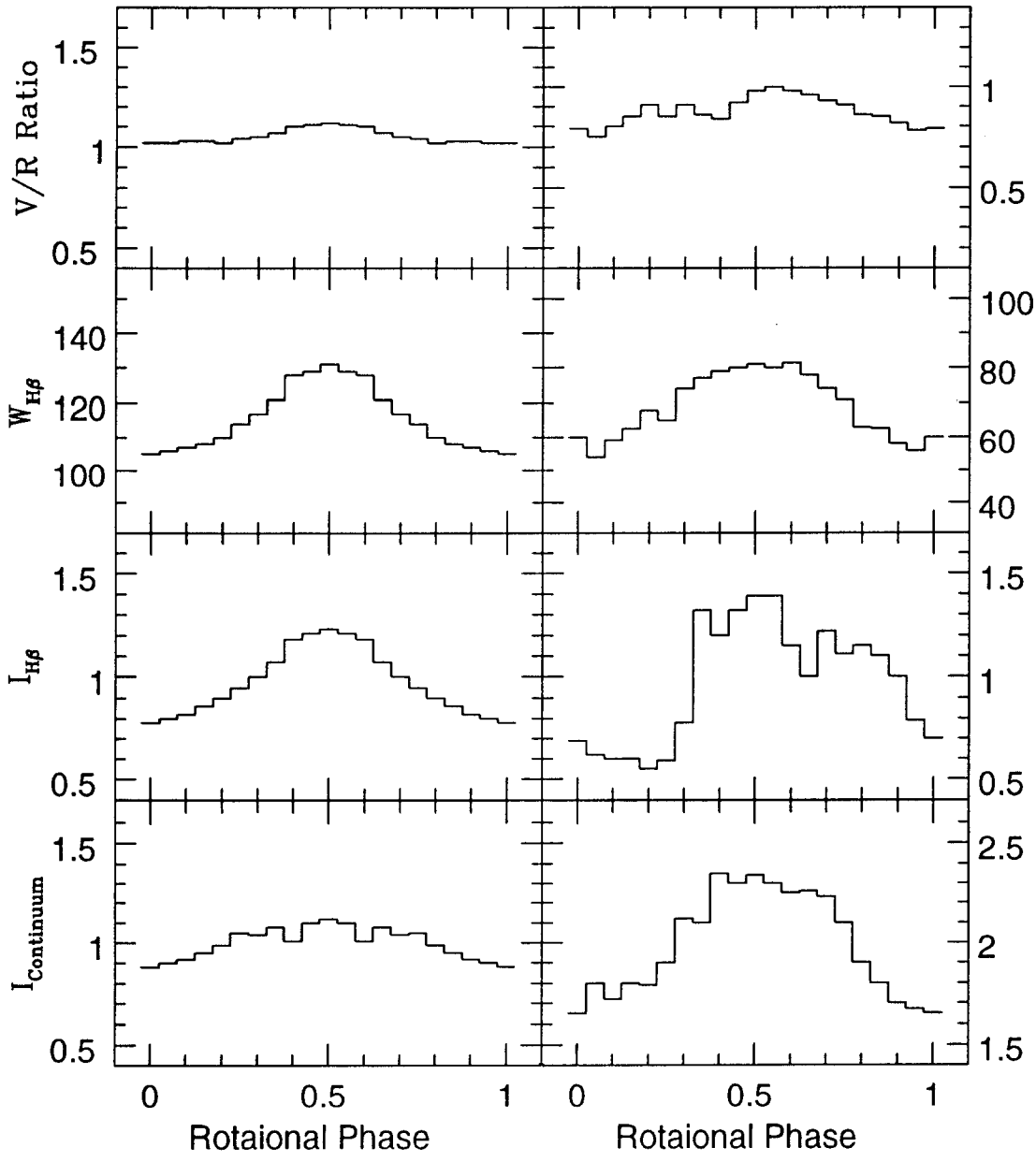

Figure 5. Calculated (left) and observed (right) optical light curves of EX Hya. The observed data are adopted from Hellier *et al.* (1987).

us an information about how the reprocessed radiation from the hot accretion funnel is distributed in the direction of the line of sight. A V/R ratio with a value less than 1 implies therefore that the observer see more material in accretion funnel flowing away from the observer than the material flowing to the observer. In addition to the calculated light curves the observed light curves of EX Hya (Hellier *et al.* 1987) are contained also in this figure showing that our model calculation explains the observed optical spectrum. More detailed discussion of these light curves can be found in Kim and Beuermann (1994a,b).

The main property of our model calculation shown above can be summarized by the argument that the energy dependence of X-ray radiation and the optical continuum and line emission can be reproduced in context of the accretion funnel model, in addition to the result providing the evidence that the light curves of X-ray, optical continuum and line emission have their maximum at the same rotational phase, namely when the upper magnetic pole is pointed away from the observer. The latter property of the light curves is also shown in the observations of some intermediate polars (Rosen *et al.* 1988, Hellier *et al.* 1991). Another important property to be mentioned is that our model can localize the each emission component. The X-ray radiation and the optical continuum are produced in the region near the magnetic pole, while the line emission comes from the optically thin outer part of the magnetosphere.

A contradictory argument originates from Kaitchuck *et al.* (1987) who concluded from the interpretation of spectro-photometric data of EX Hya that the optical continuum and X-ray radiation are produced in the accretion funnel near the surface of the white dwarf, and the optical line emission is produced not only in the accretion disc, but also in the accretion funnel, as our model results show. But in their model geometry the continuum and X-ray radiation have the maximum when the magnetic pole is pointed to the observer, because the radiation is seen by the observer without great obscuration. The line width should be great at this phase due to the accretion occuring almost along the line of sight. This discrepancy with our model result should be explained in a further detailed consideration of the model gemetry.

From X-ray satellites (EXOSAT, ROSAT, GINGA, ASCA etc) many intermediate polar have been observed in X-ray region, and will be observed in the future. There are also many optical spectro-photometric data for the intermediate polar. Regarding to this fact, it is now necessary to develope the quantitative model calculation which can be compared with the observational data to determine the some unknown physical parameters of these systems.

It is however to be recognized here that before such application, our model must

be modified and refined in some points. Because it is not well known in what amount the material accretes from the accretion disc to the upper magnetic pole and to the lower one accurately, the modelling of the accretion rate around the accretion disc must be reexamined in more detail. This problem seems to be given by Kelvin Helmholtz instability as Anzer and Börner (1980, 1982, 1983) mentioned. Another point is the consideration of the ionization of the accretion funnel. Our model calculation presented here uses the absorption cross section for neutral particles by Morrison and McCammon (1983). In fact, the ionization can not be neglected, particularly in the outer part of the magnetosphere. The photoabsorption of X-ray and the reprocessing of the absorbed X-ray energy in optical spectrum will be reconsidered by such accurate consideration of the ionization effect such as in Krollick and Kallmann (1984). It is also planned to develope a model for the orbital period dependent spectrum of X-ray and optical radiation. With such model, some unsolved properties of X-rays and optical radiation observed until now can be explained in the future.

REFERENCES

Anzer U. & Börner G. 1980, A&A, 83, 133
Anzer U. & Börner G. 1982, in High energy astrophysics and cosmology, Yang J. and Zhu C. (eds.), 294
Anzer U. & Börner G. 1983, A&A, 122, 133
Beuermann, K. 1988, Advances in Space Research, 8, 283
Ferrario L., Wickramashinghe D. T. & King A. R. 1993, MNRAS, 260, 149
Gosh P. & Lamb F. K. 1979a, ApJ, 232, 259
Gosh P. & Lamb F. K. 1979b, ApJ, 234, 296
Hellier C. Mason K. O., Rosen S. R. & Cordova F. A. 1987, MNRAS, 228, 463
Hellier C., Cropper M. S. & Mason K. O. 1991, MNRAS, 248, 233
Kaitchuck, R. H., Hantzios P. A., Kakaletris P., Honeycutt R. K. & Schlegel E. M. 1987, ApJ, 317, 765
Kim, Y. 1992, JA&SS, 9, 171
Kim, Y. & Beuermann, K. 1994a, A&A, in preperation
Kim, Y. & Beuermann, K. 1994b, A&A, in preperation
Krollick, J. H. & Kallman, T. R. 1984, ApJ, 286, 366
Kurucz, R. L. 1979, ApJS, 40, 1
Morrison, R. & McCammon, D. 1983, ApJ, 270, 119
Rosen S. R., Mason K. O. & Cordova F. A. 1988, MNRAS, 231, 549
Rosen S. R., Mason K. O., Mukai K. & Williams O. R. 1991, MNRAS, 249, 417